Published January 1, 1994

Cyclic Nucleotide-gated Channels of Rat Olfactory Receptor Cells: Divalent Cations Control the Sensitivity to cAMP

JOSEPH W. LYNCH and BERND LINDEMANN

From the Department of Physiology, Universität des Saarlandes, D-66421 Homburg/Saar, Germany

ABSTRACT cAMP-gated channels were studied in inside-out membrane patches excised from the apical cellular pole of isolated olfactory receptor cells of the rat. In the absence of divalent cations the dose-response curve of activation of patch current by cAMP had a K_M of 4.0 μM at −50 mV and of 2.5 μM at +50 mV. However, addition of 0.2 or 0.5 mM Ca^{2+} shifted the K_M of cAMP reversibly to the higher cAMP concentrations of 33 or 90 μM, respectively, at −50 mV. Among divalent cations, the relative potency for inducing cAMP affinity shifts was: Ca^{2+} > Sr^{2+} > Mn^{2+} > Ba^{2+} > Mg^{2+}, of which Mg^{2+} (up to 3 mM) did not shift the K_M at all. This potency sequence corresponds closely to that required for the activation of calmodulin. However, the Ca^{2+}-sensitivity is lower than expected for a calmodulin-mediated action. Brief (60 s) transient exposure to 3 mM Mg^{2+}, in the absence of other divalent cations, had a protective effect in that following washout of Mg^{2+}, subsequent exposure to 0.2 mM Ca^{2+} no longer caused affinity shifts. This protection effect did not occur in intact cells and was probably a consequence of patch excision, possibly representing ablation of a regulatory protein from the channel cyclic nucleotide binding site. Thus, the binding of divalent cations, probably via a regulatory protein, controls the sensitivity of the cAMP-gated channels to cAMP. The influx of Ca^{2+} through these channels during the odorant response may rise to a sufficiently high concentration at the intracellular membrane surface to contribute to the desensitization of the odorant-induced response. The results also indicate that divalent cation effects on cyclic nucleotide-gated channels may depend on the sequence of pre-exposure to other divalent cations.

INTRODUCTION

The stimulation of olfactory receptor neurons by odorants results in the formation of cAMP, which directly gates cation-conducting membrane ion channels, leading to membrane depolarization and spike initiation (for a review, see Reed, 1992). During

Dr. Lynch's present address is Garvan Institute of Medical Research, St Vincents Hospital, 384 Victoria St, Darlinghurst, New South Wales 2010, Australia.

Address reprint requests and correspondence to Dr. B. Lindemann, Department of Physiology, Universität des Saarlandes, D-66421 Homburg/Saar, Germany.

J. GEN. PHYSIOL. © The Rockefeller University Press · 0022-1295/94/01/0087/20 $2.00
Volume 103 January 1994 87–106

continuous odorant exposure, odorant-induced responses usually display a progressive attenuation, or desensitization. The mechanisms involved in this process have not yet been clearly elucidated, yet are crucial to the understanding of olfactory transduction because desensitization, by modulating the time-dependence of neuronal firing patterns, contributes to the coding of odor information (Kauer, 1987).

The cAMP-gated channels which support the odor-induced current are similar in their permeation properties to the vertebrate photoreceptor cGMP-gated channels in conducting mainly monovalent cations (Nakamura and Gold, 1987; Yau and Baylor, 1989; Frings, Lynch and Lindemann, 1992*a*), but with a significant permeability to Ca^{2+} (Nakatani and Yau, 1988; Kurahashi and Shibuya, 1990). Because the removal of extracellular Ca^{2+} dramatically prolongs the duration of these currents (Kurahashi, 1990; Kurahashi and Shibuya, 1990), it is possible that Ca^{2+} influx through cyclic nucleotide-gated (CNG) channels may contribute to signal termination. Indeed, two separate mechanisms compatible with this idea have recently been proposed. A Ca^{2+}-activated, calmodulin-dependent phosphodiesterase, which is concentrated in olfactory cilia, reduces cAMP concentration leading to channel closure (Borisy, Ronnett, Cunningham, Juilfs, Beavo and Snyder, 1992). However, phosphodiesterase inhibitors only partially remove desensitization (Firestein, Darrow, and Shepherd, 1991; Boekhoff and Breer, 1992), suggesting involvement of at least one additional mechanism.

Evidence has also been presented for a distinct inhibitory mechanism whereby Ca^{2+} influx may reduce the sensitivity of the CNG channels to cAMP in catfish olfactory neurons (Kramer and Siegelbaum, 1992). The effect was attributed to an as yet unidentified Ca^{2+}-sensitive regulatory protein. The affinity shift was not sensitive to a calmodulin inhibitor, and the time-dependent washout after patch excision was not affected by exogenous calmodulin application (Kramer and Siegelbaum, 1992). In olfactory neurons of the salamander, Zufall, Shepherd, and Firestein (1991) had previously found a strong inhibition at low Ca^{2+} concentrations. However, this effect was observed at saturating cAMP concentrations, suggesting either a far larger Ca^{2+}-dependent shift than observed by Kramer and Siegelbaum (1992), or perhaps a different inhibitory mechanism.

Ca^{2+} has also recently been reported to inhibit the cGMP affinity of the photoreceptor CNG channel. In this case, the regulatory protein was identified as calmodulin (Hsu and Molday, 1993). On the other hand, Gordon, Brautigan, and Zimmerman (1992) found that Ca^{2+} induced an increase in the cGMP affinity of these channels. This affinity shift was inhibited by a protein phosphatase inhibitor, suggesting modulation of channel function by phosphorylation.

It is not yet possible to reconcile all of these results into a simple scheme. It appears that Ca^{2+} may exert multiple actions, with different effects predominating either in different species or under different experimental conditions. In this report, we describe the inhibitory effects of divalent cations on cAMP-gated channels from olfactory cells of the rat. In accordance with Kramer and Siegelbaum (1992), we found that Ca^{2+} ions shifted the cAMP-dependence of channel activation to much higher concentrations. However, the effect was significantly different in that higher Ca^{2+} concentrations were required and it did not wash out with time in excised patches. We also found that the ability of Ca^{2+} to induce the inhibition was strongly

dependent upon the history of patch exposure to divalent cations. In particular, the inhibition was irreversibly abolished by brief pre-exposure to 3 mM Mg^{2+}, but only in the absence of Ca^{2+}. We also investigated the relative potency of different divalent cations in causing the inhibitory effect. The potency sequence was found to be similar to that required for the activation of calmodulin. Short summaries of our findings have appeared in abstract form (Lindemann, Frings, and Lynch, 1992: Lynch and Lindemann, 1992).

MATERIALS AND METHODS

Cell dissociation and electrophysiological procedures have previously been described in detail (Lynch and Barry, 1991; Frings et al., 1992*a*). Briefly, the olfactory neuroepithelium from adult rats was enzymatically dissociated using 0.022% trypsin (066-07072E, Gibco Laboratories, Grand Island, NY) in a medium without added divalent cations (Table I) and incubated for 35 min at 37°C. Epithelial pieces were then gently triturated and suspended cells were allowed to settle onto the base of a glass-bottomed recording chamber. Once settled, cells were continuously superfused by a modified Tyrode solution (Table I). Although several cell types were isolated, olfactory neurons were readily identified by their distinct bipolar shape.

TABLE I

Solutions

	NaCl	KCl	$CaCl_2$	$MgCl_2$	EGTA	EDTA	NaOH	Glucose
	Concentrations in mM							
Dissociation solution	145	5	—	—	—	—	5	10
Tyrode solution	140	5	2	1	—	—	5	10
Pipette solution	140	—	—	—	10	—	25	—
Low Ca solution	160	—	—	—	—	—	5	—
0 Ca solution	155	—	—	—	2	—	10	—
0 Ca/Mg solution	150	—	—	—	—	5	15	—

The low Ca solution was prepared without added Ca^{2+} salts. Its free Ca^{2+} concentration was near 3 μM as measured with a Ca^{2+} sensitive electrode (ETH 1001).

The 0 Ca solution had a free Ca^{2+} concentration of < 1 nM, as calculated with a K_d for EGTA-Ca^{2+} of 315 nM Ca^{2+} (Bers, 1982) for a total Ca^{2+} concentration of 3 μm.

All solutions contained 10 mM HEPES and were adjusted to pH 7.4 with NaOH.

Membrane currents were recorded using standard patch-clamp techniques (Hamill, Marty, Neher, Sakmann and Sigworth, 1981). Patch pipettes, pulled in two stages from borosilicate tubing (H15/10, Jenkons Scientific, Leighton Buzzard, Bedfordshire, UK), typically had tip resistances of 10 MOhm when filled with the standard divalent cation-free pipette solution (Table I). Cell-attached membrane patches were formed amongst the cilia on the apical knobs of visually identified olfactory neurons and detached into the inside-out configuration by brief air exposure. Patches from the apical knobs typically contained up to several hundred cAMP-activated channels with unitary conductances of 14 pS, whereas those pulled from the soma contained few, if any, cAMP-activated channels.

After formation of an inside-out patch, pipettes were moved along a narrow channel of solution to a separate compartment, into which up to 12 different solutions flowed through adjacently-placed tubes. Pipette tips were placed near the outflow of each tube by moving the microscope stage. When necessary to ascertain the sequence of exposure, the flow from certain tubes was stopped. Current-voltage ($I[V]$) relationships were measured by applying digitally-

generated voltage ramps of 1-s duration in both directions and averaging the responses to (usually) eight ramps. Divalent cations normally reduced the background conductance of the patch in a reversible, concentration-dependent manner. Therefore, for each concentration of each divalent cation (see Table I), the cAMP-gated current was measured as the difference in current responses to voltage ramps applied in the presence and the absence of cAMP.

All patches were excised into Tyrode solution, then transiently exposed to a divalent cation-free solution (0 Ca solution [see Table I]), containing 100 μM cAMP to test for the presence of CNG channels, before commencement of the experiment. Patches exposed only to these solutions are described as naive. Divalent cation sequence protocols were then applied as described in the Results.

The solutions are summarized in Table I. In general, responses were measured under conditions of symmetrical [NaCl]. The patch pipette solution was used in all experiments. The 0 Ca solution (2 mM EGTA and no added Ca^{2+}) was used to measure responses in the absence of Ca^{2+}. Responses at different Ca^{2+} concentrations were measured using the low Ca solution (3 μM Ca^{2+} when no Ca^{2+} was added) or a Ca solution, where $CaCl_2$ was added to the low Ca solution to the concentration indicated. Responses to all other divalent cations (Mg^{2+}, Ba^{2+}, Co^{2+}, Mn^{2+}, Sr^{2+}) were measured in 0 Ca solution, with the chloride salt of the relevant divalent cation added to give the concentration indicated. The Na^+ salt of cAMP (Sigma Chemical Co., St Louis, MO) was used in all experiments.

All voltages are expressed as potential of the internal with respect to the external membrane surface. Experiments were performed at room temperature (20–22°C).

RESULTS

Micromolar Concentrations of Ca^{2+} Do Not Decrease the cAMP-dependent Current in the Rat

Recent results obtained with membrane patches excised from catfish olfactory cells indicate that Ca^{2+} on the cytosolic side of the membrane inhibits the cAMP-induced current with a half-maximal effect near 3 μM (Kramer and Siegelbaum, 1992). We attempted to reproduce this effect, using inside-out membrane patches excised from apical knobs of rat olfactory receptor neurons. In Fig. 1 *A*, the cAMP dose-response measured in the presence of 3 μM [Ca^{2+}] (*circles*) is compared with results from an earlier study performed under identical conditions (Frings et al., 1992*a*), but where [Ca^{2+}] was <10 nM (*curves*). There was no significant difference in the sensitivity to cAMP.

Another possibility, inferred from the data of Zufall et al. (1991), is that 3 μM [Ca^{2+}] may inhibit the current by a mechanism unrelated to a shift in the cAMP sensitivity. To test this possibility, $I(V)$s were measured in different [Ca^{2+}] in the presence of a saturating concentration (100 μM) of cAMP. As displayed in Fig. 1 *B*, decreasing the free Ca^{2+} concentration from 3 μM to <3 nM by the progressive addition of EGTA, had no noticeable effect. A similar result was obtained with each of three patches.

Thus, we were unable to reproduce in rat olfactory cells the inhibitory effect of Ca^{2+} at the same concentration as has been reported in the salamander or catfish. Although the dose-response experiments (Fig. 1 *A*) were completed within 5 min after patch excision, it is possible that the lack of effect may have been attributable to the rapid washout of a cytosolic factor.

Inhibition of cAMP-dependent Current by Divalent Cations at Higher Concentrations

When cAMP concentrations of 1, 3, 10, and 100 μM were sequentially applied to the cytosolic side of a membrane patch in the absence of Ca^{2+}, the $I(V)$ relationships in Fig. 2 *A* (*upper left*) were generated. The apparent dissociation constant (K_M) for cAMP was near 3 μM. When repeated in the presence of 0.5 mM Ca^{2+} (Fig. 2 *A*, *lower left*), the current magnitudes were decreased in a manner which depended on the concentration of cAMP. Similar behavior was observed in each of five patches.

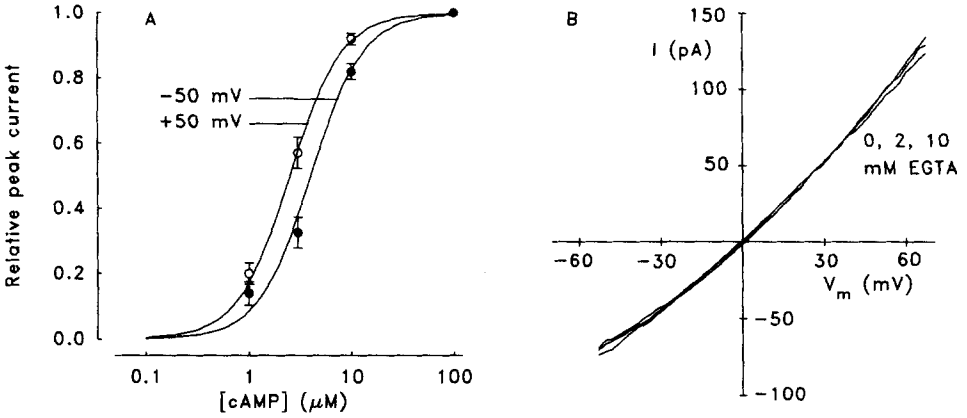

FIGURE 1. Low concentrations of Ca^{2+} (near 3 μM) are without effect on the activation of channels by cAMP. In this and all subsequent figures, the $I(V)$ relationships show difference currents obtained in the presence and absence of cAMP, for each divalent cation condition. (*A*) Dose-responses for cAMP at +50 (*hollow circles*) and −50 mV (*filled circles*) averaged from seven inside-out patches exposed to 0 Ca solution (see Table I), having a free $[Ca^{2+}]$ of < 1 nM. Error bars represent SEM. The sigmoid curves represent the corresponding best fits to dose-responses averaged from seven patches measured in low Ca solution (free $[Ca^{2+}] \sim 3$ μM) reproduced from Frings et al. (1992). The fitted curves had Hill coefficients of 1.8 and K_M values of 2.5 μM (+50 mV) and 4.0 μM (−50 mV). (*B*) $I(V)$ curves obtained from one inside-out patch in the presence of 100 μM cAMP, showing that the addition of 2 or 10 mM EGTA to the low Ca solution had no effect. The three superimposed curves were obtained upon exposure to low Ca solution (no EGTA), 0 Ca solution (2 mM EGTA) and 10 mM EGTA solution. The latter contained (in mM): NaCl 160, EGTA 10, NaOH 25 (pH 7.4). Equivalent results were obtained with two other patches.

The inhibitory effect of Ca^{2+} is highlighted by plotting the ratios of currents recorded for [cAMP]s of 3, 10, and 100 μM in the presence of 0.5 mM Ca^{2+} with respect to those measured in the absence of Ca^{2+}. Fig. 2 *A* (*right*) shows such ratio plots averaged from five patches. Although some Ca^{2+}-induced suppression occurred at all [cAMP]s, it was progressively overcome at higher cAMP concentrations. Corresponding results were reported for the cGMP-gated channel of the tiger salamander photoreceptor (Colamartino, Menini, and Torre, 1991).

When a similar experiment was performed using 0.5 mM Mg^{2+} instead of Ca^{2+}, the results were different. In the example shown in Fig. 2 *B*, 0.5 mM Mg^{2+} induced a strongly voltage-dependent block, but the ratio plots of current recorded in the

Published January 1, 1994

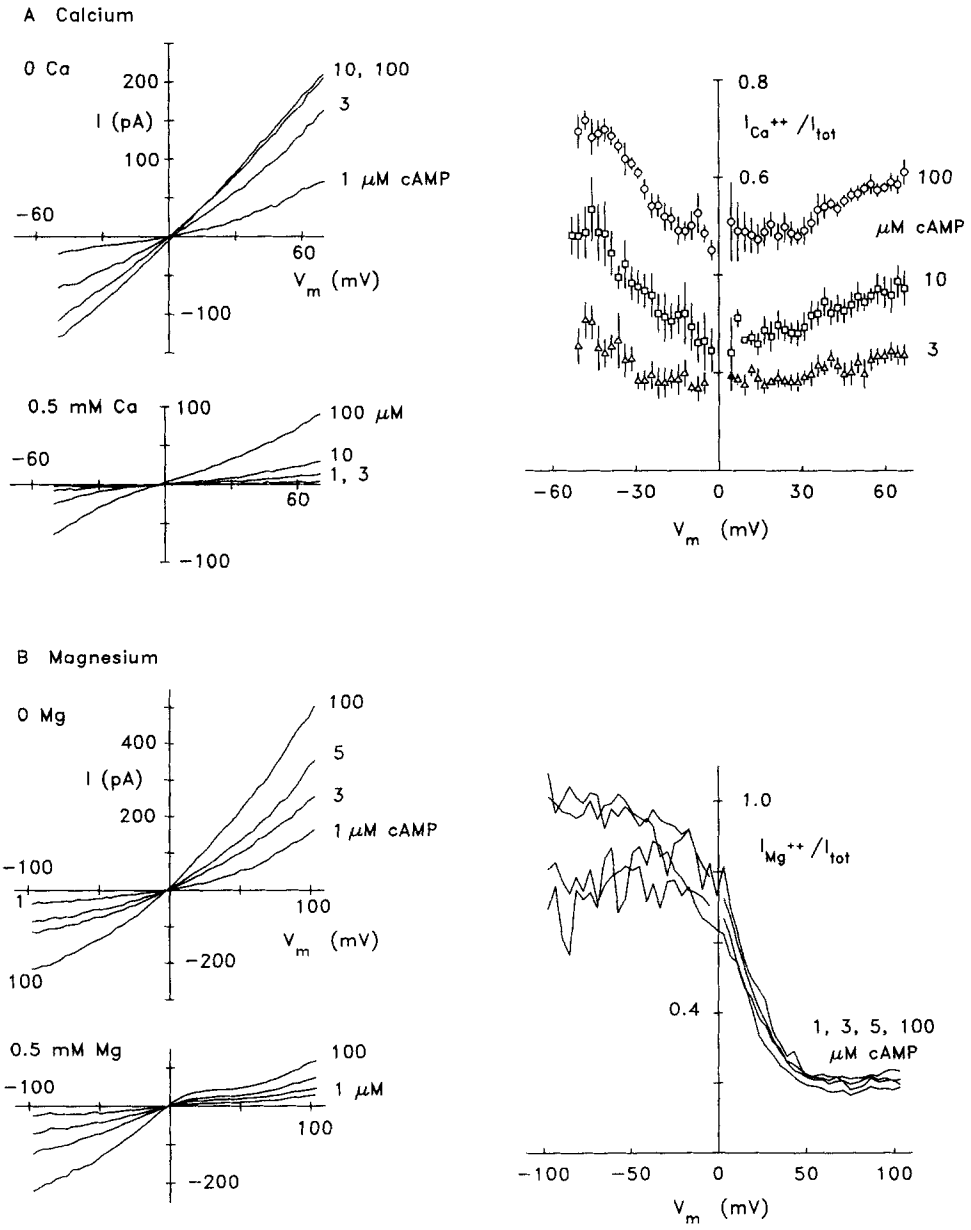

FIGURE 2. The relative current-inhibition caused by Ca^{2+} appears to depend on [cAMP], while that caused by Mg^{2+} does not. (*A*) The upper left panel displays a series of $I(V)$ relationships for cAMP of 1, 3, 10, and 100 μM in the absence of Ca^{2+}. In the lower left panel, the experiment was repeated after $[Ca^{2+}]$ had been increased to 0.5 mM (same patch). The right panel shows current inhibition ratios, i.e. current values recorded in the presence of 0.5 mM $[Ca^{2+}]$ divided by those obtained at 0 mM $[Ca^{2+}]$. Inhibition ratios for cAMP concentrations of 3, 10, and 100 μM are shown as triangles, squares and circles (averaged from five patches). (*B*) Similar experiment to *A*, but using 0.5 mM $[Mg^{2+}]$ instead of 0.5 mM $[Ca^{2+}]$. All data from the same patch. Left panels: examples of $I(V)$ relationships generated in response to cAMP concentrations of 1, 3, 5 and 100 μM in the absence (*upper*) and presence (*lower*) of 0.5 mM $[Mg^{2+}]$. (*Right*) Current inhibition ratios of the data displayed in the left panel, indicating a lack of dependence on [cAMP].

presence with respect to the absence of 0.5 mM Mg^{2+} were not consistently affected by [cAMP]. This was confirmed in each of four patches. For the photoreceptor CNG channel, Colamartino et al. (1991) found a different behavior, i.e., that the Mg^{2+}-induced suppression had a similar [cGMP]-dependence to that seen for Ca^{2+}.

To explain this interaction between Ca^{2+} and cyclic nucleotide effects, it was suggested that a higher cyclic nucleotide concentration opens the channel to a larger conductance state, thereby facilitating Ca^{2+} permeation and reducing the effectiveness of a supposed pore blocking effect of Ca^{2+} (Colamartino et al., 1991; Kaupp and Koch, 1992). However, as described in the next section, this effect can be explained by Ca^{2+}-dependent inhibition of the activation of the channels by cAMP.

Ca^{2+} Decreases Sensitivity to cAMP

The possibility that Ca^{2+} may modulate the sensitivity of the channels to activation by cAMP was tested by measuring the cAMP dose-responses in the presence of 0.5 mM Ca^{2+}. One example of such an experiment is shown in Fig. 3 *A* (*left*). Compared to Fig. 2 *A*, where 3 μM cAMP caused about half-maximal activation, a more than 10-fold higher [cAMP] was now needed. The right panel shows cAMP dose-responses averaged from currents recorded in five patches in 0.5 mM Ca^{2+} (*squares*), at both +50 mV (*hollow squares*) and −50 mV (*filled squares*). Both dose-responses were fitted by curves with a Hill coefficient of 1.7 and K_M values of 55 μM at +50 mV and 90 μM at −50 mV. The cAMP dose-response obtained in the absence of divalent cations is also included for comparison (Fig. 3 *A, circles*), using data replotted from Frings et al. (1992*a*). These data were fitted with a Hill coefficient of 1.8 and K_M values of 2.5 μM (+50 mV, *hollow circles*) and 4.0 μM (−50 mV, *filled circles*), respectively. K_M values are indicated on the abscissa of each dose-response plot.

These results show a marked increase in the K_M for cAMP caused by the presence of 0.5 mM Ca^{2+}. A lower [Ca^{2+}] of 0.2 mM caused a less pronounced inhibition, as will be discussed below. During continuous exposure to a solution of constant [Ca^{2+}], time-dependent shifts in the K_M for cAMP were never observed. Furthermore, the Ca^{2+}-dependent inhibition was completely and rapidly reversed as Ca^{2+} was added or removed. The effect indicates that Ca^{2+} present at the internal surface of the membrane causes desensitization of the channels with respect to their agonist. The shift of the K_M must have contributed strongly to the apparent interaction between Ca^{2+} and cAMP as represented in Fig. 2 *A* and suggests that a similar effect may also exist for photoreceptor CNG channels (Colamartino et al., 1991).

The relative abilities of Mg^{2+}, Ba^{2+}, Sr^{2+}, and Mn^{2+} to inhibit cAMP-induced current activation were also examined. Unlike Ca^{2+}, none of these cations had any effect at concentrations of 0.5 mM at the cytosolic membrane surface. Therefore, their relative effectiveness was compared at concentrations of 3 mM. The effect of 3 mM Mg^{2+} is demonstrated in Fig. 3 *B*. The $I(V)$ curves show a strong voltage-dependent block, reminiscent of the Mg^{2+} effect at inward rectifier K^+ channels (reviewed in Jan and Jan, 1992). However, 3 mM Mg^{2+} had no clear effect on the K_M for cAMP. The cAMP dose-response was fitted by a Hill coefficient of 1.6 and with a K_M of 2.0 μM at +50 mV (*filled circles*) and 5.8 μM at −50 mV (*hollow circles*). These values were not significantly different from those determined in the absence of divalent cations.

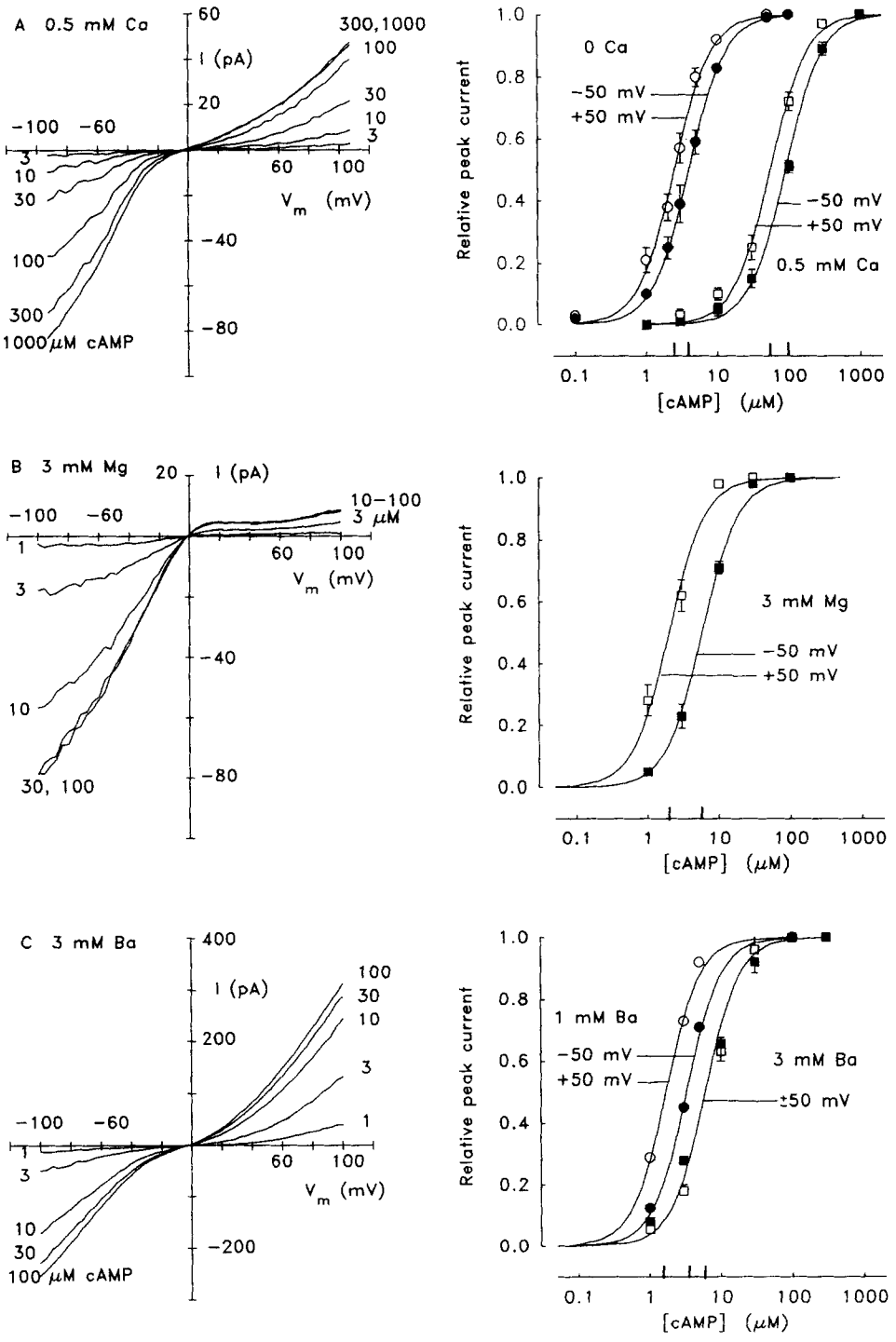

FIGURE 3.

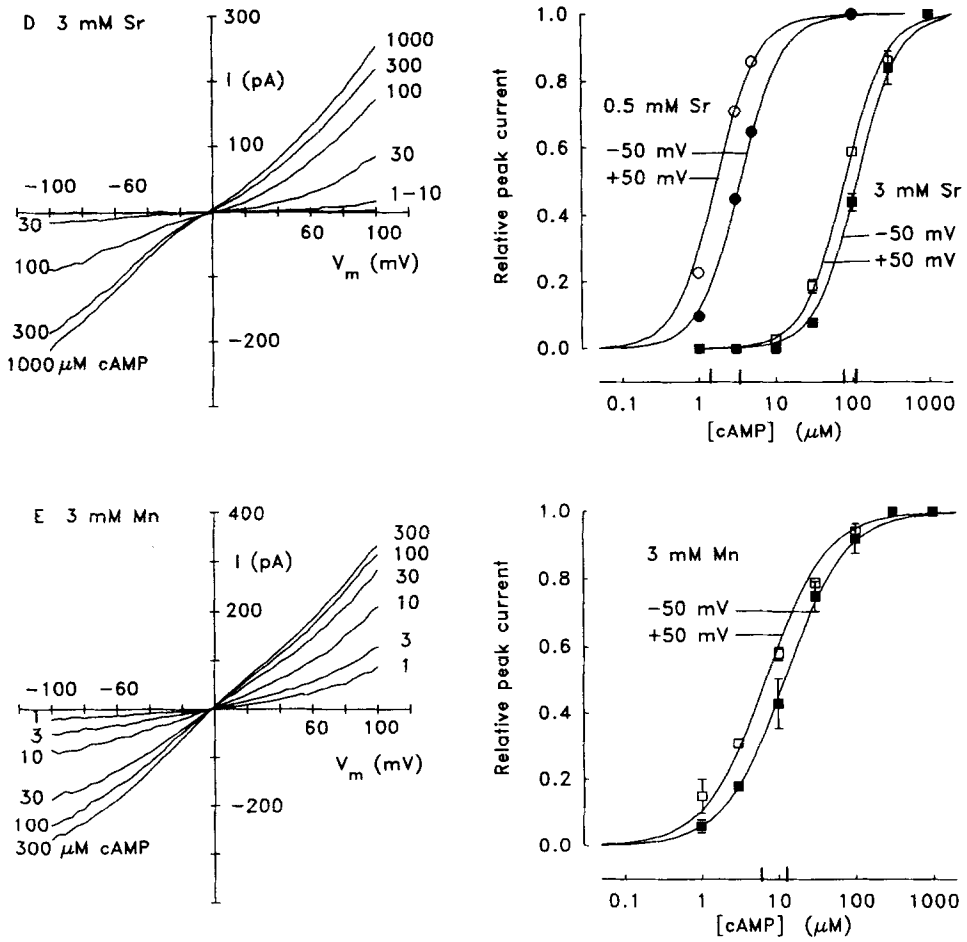

FIGURE 3. The effects of Ca^{2+}, Mg^{2+}, Ba^{2+}, Sr^{2+}, and Mn^{2+} on the cAMP dose-response. For each divalent cation, cAMP dose-responses were obtained from $I(V)$ curves, using currents at +50 and −50 mV. Because divalent cations also caused a direct channel block, the 'relative peak currents' are the currents normalized with respect to the maximum observed in each divalent cation condition. Unless otherwise indicated, each point represents data averaged from multiple patches and error bars (±SEM) are shown when larger than symbol size. K_M values are indicated as short lines on the [cAMP] scales. (*A*) The left panel shows a typical sequence of $I(V)$ relationships recorded in one patch at the indicated [cAMP] in the presence of 0.5 mM Ca^{2+}. The right panel shows averaged cAMP dose-responses in both the absence of Ca^{2+} (*circles*) and in 0.5 mM Ca^{2+} (*squares*). The data for 0 Ca^{2+} were replotted from Fig. 2 *F* of Frings et al. (1992*a*), with the fitted curves having a Hill coefficient of 1.8 and K_M values of 2.5 μM (+50 mV) and 4.0 μM (−50 mV). Data were averaged from eight patches. The data for 0.5 mM Ca^{2+} were averaged from five patches, with the fitted curves having a Hill coefficient of 1.7 and a K_M of 55 μM (+50 mV) and 90 μM (−50 mV). (*B*) The left panel shows an example of $I(V)$ relationships activated by the indicated [cAMP] in the presence of 3 mM Mg^{2+}. The right panel shows the dose-response averaged from two patches, with fitted curves having a Hill coefficient of 1.6 and a K_M of 2.0 μM (+50 mV) and 5.8 μM (−50 mV). (*C*) The left panel shows an example of $I(V)$ relationships activated by the indicated cAMP in 3 mM Ba^{2+}. The right panel

In the presence of 3 mM Ba^{2+}, a slight increase in the K_M was observed (Fig. 3 *C, squares*) although there was no effect at a concentration of 1 mM (*circles*). The voltage-dependence of cAMP activation was diminished in 3 mM Ba^{2+}, both +50 and −50 mV having a K_M of 6.0 μM. However, the Hill coefficient remained unchanged. In 3 mM Sr^{2+} , a dramatic increase in K_M was observed (Fig. 3 *D, squares*), while 0.5 mM Sr^{2+} did not elicit this effect (*circles*). The cAMP dose-response in 3 mM Sr^{2+} was fitted with a K_M of 80 μM at +50 mV (*filled squares*) and 115 μM at −50 mV (*hollow squares*), and a Hill coefficient of 1.6. In 3 mM Mn^{2+}, the cAMP dose-response was shifted to a value of 6 μM at +50 mV (Fig. 3 *E, filled squares*) and 12 μM at −50 mV (*hollow squares*). It also reduced the apparent Hill coefficient from 1.8 to 1.1.

Because Ca^{2+} was the only divalent cation to be effective at 0.5 mM, the relative potencies for inhibiting the cAMP-induced activation may be assigned as follows:

$$Ca^{2+} > Sr^{2+} > Mn^{2+} > Ba^{2+} > Mg^{2+}.$$

When plotted as a function of ionic radius, this sequence forms a pyramid-shaped distribution, with Ca^{2+} at the apex. Thus, the closer the ionic radius to Ca^{2+}, the better the divalent cation acts as a substitute for Ca^{2+}. Clearly, the abilities to block the channel and to shift cAMP sensitivity are distributed differently. For example, Mg^{2+} is an efficient channel blocker but the poorest shifter.

It was recently reported that low (μM) concentrations of Ca^{2+} dramatically sensitized the photoreceptor cGMP-gated channel to activation by cGMP (Ildefonse and Bennett, 1991). In the present study we were unable to demonstrate any effect of Ca^{2+} at concentrations of 10 μM (n = 2), 100 μM (n = 3) or 1 mM (n = 3).

cAMP Affinity Shifts Were Abolished by Pre-exposure to Mg^{2+}

Exposure of the cytosolic surface of an inside-out patch to Mg^{2+} prevented a subsequent K_M shift induced by the first divalent cation. An example of this is given in Fig. 4, where the sequence of divalent cation exposure was:

$$3 \text{ mM } Sr^{2+}/3 \text{ mM } Mg^{2+}/3 \text{ mM } Sr^{2+}.$$

The first exposure of the newly-excised (or naive) patch to 3 mM Sr^{2+} caused the K_M to be shifted to near 100 μM (Fig. 4 A), where it remained stable while the exposure

---

shows averaged cAMP dose-responses measured in 1 mM Ba^{2+} (*circles*) and 3 mM Ba^{2+} (*squares*). The data for 1 mM Ba^{2+} were averaged from four patches and fitted curves have a Hill coefficient of 1.6 with a K_M of 1.5 μM (+50 mV) and 3.3 μM (−50 mV). The data for 3 mM Ba^{2+} were averaged from two patches with the fitted curve having a Hill coefficient of 1.8 and a K_M of 6.0 μM. (*D*) The left panel shows an example of $I(V)$ relationships activated by the indicated [cAMP] in 3 mM Sr^{2+}. The right panel shows cAMP dose-responses recorded in 0.5 mM Sr^{2+} (*circles*) and 3 mM Sr^{2+} (*squares*). The data for 0.5 mM Sr^{2+} were from one patch and fitted with a Hill coefficient of 1.8 and a K_M of 1.5 μM (+50 mV) and 3.5 μM (−50 mV). The data for 3 mM Sr^{2+} were averaged from two patches and fitted curves had a Hill coefficient of 1.6 and a K_M of 80 μM (+50 mV) and 115 μM (−50 mV). (*E*) The left panel shows an example of $I(V)$ relationships activated by the indicated cAMP in 3 mM Mn^{2+}. The right panel shows the cAMP dose-response averaged from two patches, with the fitted curve having a low Hill coefficient (1.15) and a K_M of 6 μM (+50 mV) and 12 μM (−50 mV).

to 3 mM Sr^{2+} was continued for 20 min (Fig. 4 *B*). After brief exposure (2 min) to a solution containing 3 mM Mg^{2+} as the only divalent cation (Fig. 4 *C*), the K_M subsequently measured in 3 mM Sr^{2+} (after the removal of Mg^{2+}) was near the value typically seen in the absence of divalent cations (Fig. 4 *D*). This K_M remained constant, during the continued exposure to 3 mM Sr^{2+}, for the following 90 min (Fig. 4 *E*). The time courses of three relevant parameters are given in *F–H*. After the transient exposure to Mg^{2+}, there was a ~20% stepwise reduction in the maximum current (*F*). However, this decrease was not observed in all patches and was not studied in detail. Immediately after Mg^{2+} exposure, the K_M decreased to < 1/10th of its previous value (*G*). The Hill coefficient remained unchanged (*H*). As shown below, Mg^{2+} pre-exposure also abolished the Ca^{2+}-induced cAMP affinity shifts.

The inhibitory effect of Mg^{2+} was further investigated using 0.2 mM Ca^{2+}, which also induced a large K_M shift. An example of $I(V)$ relationships recorded from one patch at increasing [cAMP] are given in Fig. 5 *A*, and dose-responses averaged from four patches are shown in Fig. 5 *C*. At −50 mV, the addition of 0.2 mM Ca^{2+} increased the cAMP affinity from 4 to 33 μM. In Fig. 5 *B*, it is apparent that exposure for 60 s to a solution containing both Mg^{2+} and Ca^{2+} had no effect on the cAMP sensitivity. This experiment represents the following sequence:

$$0.2\text{ mM } Ca^{2+}/(3\text{ mM } Mg^{2+} + 0.2\text{ mM } Ca^{2+})/0.2\text{ mM } Ca^{2+}.$$

This negative result was confirmed in three other patches. Yet, as demonstrated below, exposure for 60 s to a solution containing 3 mM Mg^{2+} and no Ca^{2+} completely abolished the desensitising K_M shift induced by 0.2 mM Ca^{2+}. Thus, the continuous presence of 0.2 mM Ca^{2+} effectively eliminates the ability of Mg^{2+} to prevent Ca^{2+}-induced K_M increases. This suggests why patch excision into bath Tyrode (which contained 2 mM Ca^{2+} and 1 mM Mg^{2+}) did not prevent subsequent shifts of K_M.

From Fig. 4, it cannot be concluded whether Mg^{2+} induced a general increase in the sensitivity to cAMP, or whether it abolished the K_M shift induced by Sr^{2+}. Using 0.2 mM Ca^{2+} instead of 3 mM Sr^{2+} to induce the shift, the following exposure sequence was used to distinguish between these two possibilities:

$$0\text{ divalent}/0.2\text{ mM } Ca^{2+}/3\text{ mM } Mg^{2+}/0\text{ divalent}/0.2\text{ mM } Ca^{2+}.$$

An example of such an experiment is given in Fig. 6. In Fig. 6, *A* and *B*, it is clear that a 60-s pre-exposure to 3 mM Mg^{2+} had no effect on the cAMP dose-response measured in the absence of divalent cations, although in the same patch (Fig. 6, *C–E*) it completely abolished the K_M shift induced by 0.2 mM Ca^{2+}. Similar results were obtained in two other patches. To average results from different patches, the ratio of currents obtained with 10 with respect to 100 μM cAMP was chosen as an assay of a desensitising K_M shift because 10 μM cAMP is almost saturating in a zero divalent solution, but near half maximal in 0.2 mM Ca^{2+}. This ratio, which was measured at −50 mV, is termed $I_{10/100}$. The $I_{10/100}$ in zero divalent solution, averaged from three patches, was 0.87 ± 0.03 (±SEM, $n = 3$). Addition of 0.2 mM Ca^{2+} reduced $I_{10/100}$ to 0.46 ± 0.09. Subsequent exposure to 3 mM Mg^{2+} for 60 s increased this ratio to 0.85 ± 0.06, which was not significantly different from control. No significant shift in the zero divalent cation cAMP dose-response was measured in any of the three

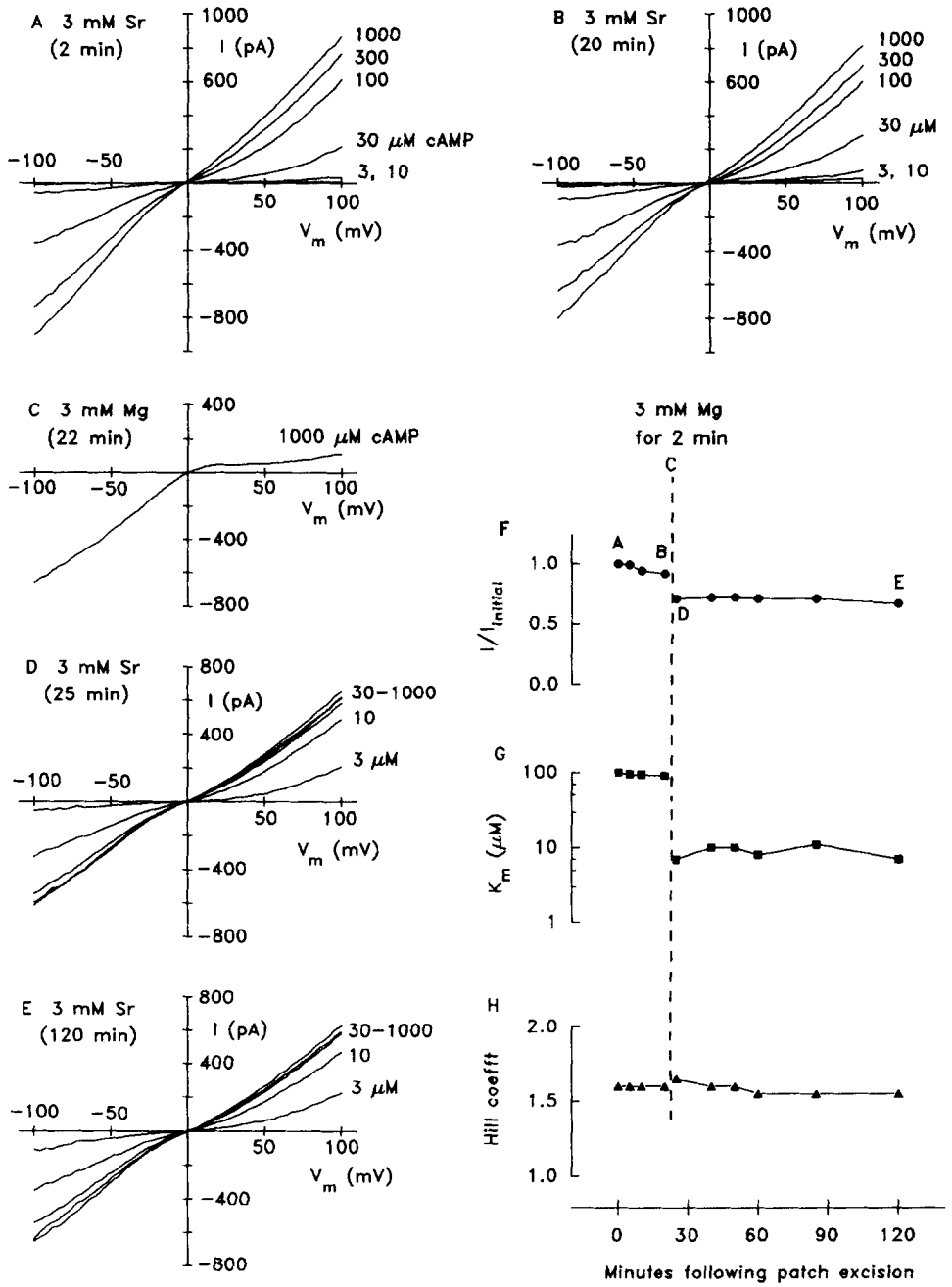

FIGURE 4. The decrease in the cAMP sensitivity, induced in this case by 3 mM Sr^{2+}, is abolished following a 2-min exposure to 3 mM Mg^{2+}. Data from 1 patch. *I(V)* relationships activated by the indicated [cAMP] in 3 mM Sr^{2+} are displayed for the following times after patch excision: 2 min (*A*), 20 min (*B*), 25 min (*D*) and 120 min (*E*). At 22 min (*C*), the patch was exposed for 2 min to a solution containing 3 mM Mg^{2+} and 1 mM cAMP. Eight 1-s voltage ramps between −100 and +100 mV were also applied during this period. Thereafter, the Mg^{2+}

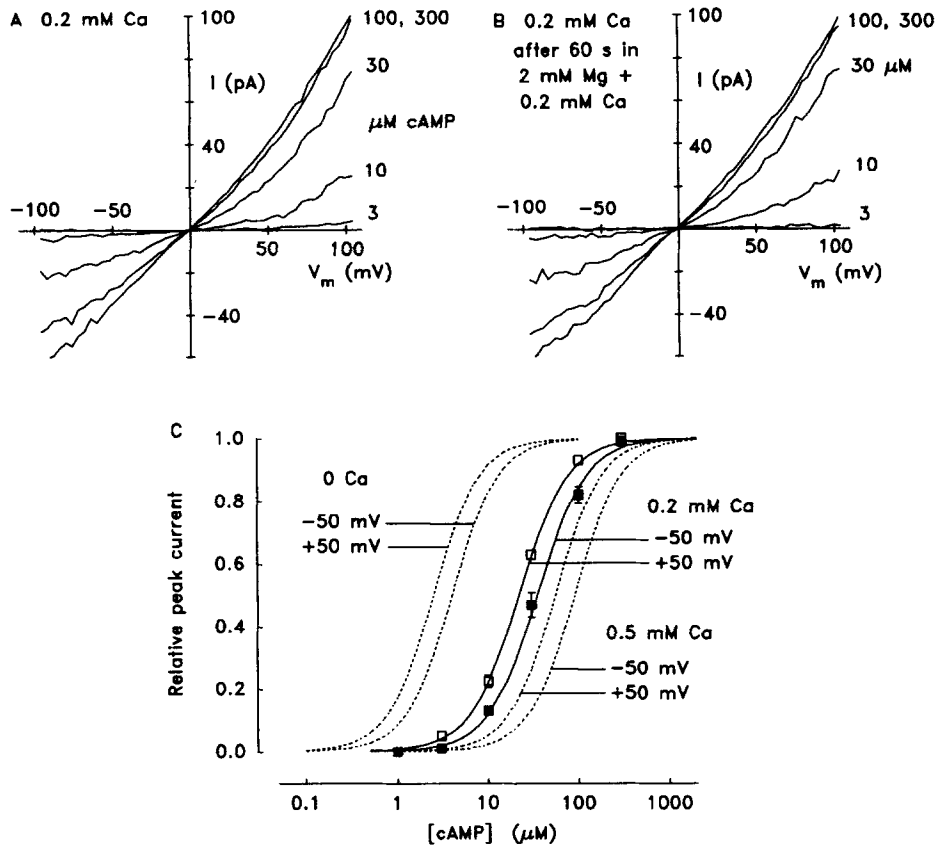

FIGURE 5. The cAMP dose-response shift induced by the lower $[Ca^{2+}]$ of 0.2 mM. An example of a cAMP dose-response in 0.2 mM Ca^{2+} before (*A*) and after (*B*) exposure of the patch to a solution (low Ca solution in Table I) containing 2 mM Mg^{2+} + 0.2 mM Ca^{2+} for 60 s. (*C*) The dose-responses of cAMP at +50 mV (*hollow squares*) and −50 mV (*filled squares*) were averaged from four patches. Error bars (±SEM) are displayed when larger than symbol size. The fitted curves had a Hill coefficient of 1.6 and a K_M of 22 μM (+50 mV) or 33 μM (−50 mV). Corresponding cAMP dose-responses for 0 and 0.5 mM Ca^{2+} from Fig. 2 *A* (*dashed lines*) are included for comparison.

patches. Thus, the effect of Mg^{2+} was simply to abolish the affinity shift induced by 0.2 mM Ca^{2+}.

Because the protective effect of Mg^{2+} required the absence of Ca^{2+}, it is possible that either, (*a*) both Mg^{2+} and Ca^{2+} compete for a site (or sites) at which only Mg^{2+} is

was washed away. Data in *A–E* represent sample recordings. A summary of all cAMP dose-responses measured in this patch, plotted as a function of time following patch excision, is presented in *F, G,* and *H*. (*F*) Ratio of current activated by saturating cAMP at indicated time following patch excision, measured with respect to the current activated by saturating cAMP at time t = 120 s. (*G*) The K_M of the cAMP dose-response recorded at −50 mV. (*H*) Hill coefficient of the cAMP dose-response.

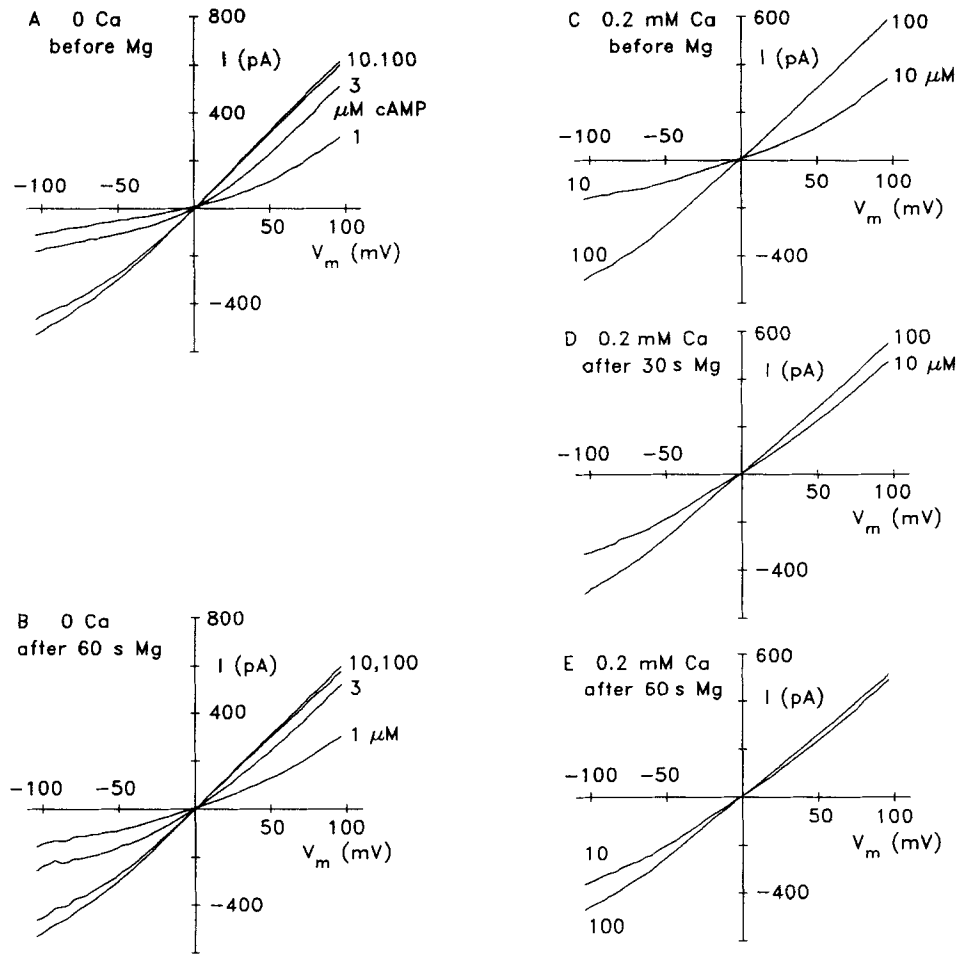

FIGURE 6. Protection from channel desensitization: effect of 3 mM Mg^{2+} on the cAMP dose-responses in 0 and 0.2 mM Ca^{2+}. (*A* and *B*) Dose-response in 0 Ca^{2+} before (*A*) and after (*B*) a 60-s application of 3 mM Mg^{2+}. (*C–E*) *I(V)* relationships recorded in 10 and 100 μM cAMP in the presence of 0.2 mM Ca^{2+} before (*C*), after 30 s (*D*), and after 60 s (*E*) exposure to 3 mM Mg^{2+}. All data are from the same patch. In these experiments, neither voltage ramps nor the addition of cAMP significantly increased the rate of induction of the Mg^{2+} effect ($n = 2$ each). Furthermore, the Mg^{2+} effect was not reversed by exposure to a strongly Mg^{2+} chelating solution, containing 2 mM EDTA ($n = 2$).

effective but for which it has a lower affinity than Ca^{2+}, or (*b*), before Mg^{2+} can be effective, the desensitising shift must be reversed by removal of Ca^{2+}. These can be tested by observing whether a higher [Ca^{2+}] can protect against a shift caused by a lower [Ca^{2+}]. The following exposure sequence was used:

$$0.2 \text{ mM } Ca^{2+}/3 \text{ mM } Ca^{2+}/0.2 \text{ mM } Ca^{2+}.$$

Before exposure to 0.2 mM Ca^{2+}, the $I_{10/100}$ was 0.81 ± 0.02 (±SEM, $n = 2$), which reduced to 0.37 ± 0.12 upon exposure to 0.2 mM Ca^{2+}. After exposure to 3 mM

Ca^{2+} for 2 min, the $I_{10/100}$ increased to 0.81 ± 0.05. The K_M in the absence of divalent cations did not change. Thus, 3 mM Ca^{2+} protected against the desensitising shift induced by 0.2 mM Ca^{2+}, suggesting that shifting sites are functionally distinct from the protection sites, but that higher divalent concentrations are necessary for activation of protection sites. The longer time required to establish the protective effect of Ca^{2+} (120 s, c.f., 60 s for Mg^{2+}) may indicate a relatively reduced affinity for the protection site.

Because the K_M shift induced by 0.2 mM Ca^{2+} was abolished by a subsequent exposure to 3 mM Mg^{2+}, it may be anticipated that reversing the exposure sequence would have the same effect. That is, exposure of a naive patch to 3 mM Mg^{2+} should prevent a K_M shift induced by a subsequent exposure to 0.2 mM Ca^{2+}. This was tested using the following exposure sequence:

3 mM Mg^{2+}/0 divalent/0.2 mM Ca^{2+}/3 mM Mg^{2+}/0.2 mM Ca^{2+}.

Immediately after excision into normal Tyrode solution, patches were exposed to 3 mM Mg^{2+} solution for 120 s. In each of three patches tested, the cAMP dose-response measured in the absence of divalent cations was normal and did not change throughout the experiment. But surprisingly, after a 120-s pre-exposure to 3 mM Mg^{2+}, the usual desensitising K_M shift was observed upon exposure to 0.2 mM Ca^{2+}. The $I_{10/100}$ was originally 0.82 ± 0.04 (n = 3) and reduced to 0.42 ± 0.10 in 0.2 mM Ca^{2+}. Then, after re-exposure to 3 mM Mg^{2+}, the removal of the Ca^{2+}-induced K_M shift occurred as before. Thus, pre-exposure of naive patches to Mg^{2+} was ineffective in preventing the Ca^{2+}-induced K_M shift.

DISCUSSION

Summary of Results

Ca^{2+}, acting at the cytosolic membrane surface, decreased the sensitivity of the CNG channels to activation by cAMP. The sensitivity decrease could also be achieved with other divalent cations, with a relative potency dependent on the closeness of the ionic radius to Ca^{2+}. Mg^{2+} was the only divalent cation tested which did not cause a shift. Once a shift had been induced by simultaneous exposure to cAMP and a shifting divalent cation, brief transient exposure to a relatively high (3 mM) concentration of Ca^{2+}, Mg^{2+}, or Ba^{2+} (not shown) protected against subsequent shifts. Surprisingly, mixtures of divalent cations were not effective in achieving this protection. Our results can be summarized by the reaction scheme in Fig. 7. To simplify discussion of this scheme, only Ca^{2+} is considered as a shifting divalent cation and Mg^{2+} is considered as a protecting divalent. In this model, the term protection is used descriptively and is not intended to suggest a physical action of Mg^{2+}.

The conversion from the high affinity (R') to the low affinity (R^S) state was rapidly achieved by the addition of 0.2 mM Ca^{2+}. It was readily reversible upon removal of Ca^{2+}, did not wash out with time in excised patches (e.g., Fig. 4, *A* and *B*) and was independent of the presence of 3 mM Mg^{2+} (Fig. 5, *A* and *B*). However, once Ca^{2+} was removed from the solution, 3 mM Mg^{2+} induced the apparently irreversible reaction to state (R'') where desensitising shifts could no longer be induced. This step did not require cAMP. Surprisingly, this reaction ($R' \rightarrow R''$) could not be induced in

naive patches which had been pre-exposed only to bath Tyrode solution (containing 2 mM Ca^{2+} and 1 mM Mg^{2+}) and to a zero divalent solution containing 100 μM cAMP. Apparently, the R^S state had first to be achieved before Mg^{2+} exposure was effective. Thus, it was necessary to define an additional state (R), corresponding to that of naive patches. The step $R \rightarrow R^S$ required both Ca^{2+} and cAMP, while Mg^{2+} was optional. It was not established whether excision into bath Tyrode induced any changes in the channels from their state in the intact cell.

Comparison with Other Studies

This report confirms a recent study where Ca^{2+} was shown to reduce the sensitivity of catfish olfactory CNG channels to activation by cAMP (Kramer and Siegelbaum,

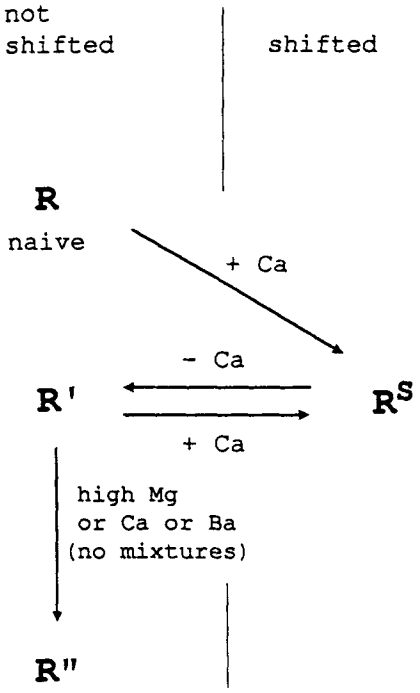

FIGURE 7. Scheme of possible transitions to explain divalent cation–cAMP interactions. In state R^S the cAMP-dose response was shifted to higher K_M values (channel desensitization). The transition $R \rightarrow R^S$ was achieved by exposure to cAMP + Ca^{2+} (with and without Mg^{2+}), whereas cAMP + Mg^{2+}, Ca^{2+} + Mg^{2+}, cAMP alone, or Mg^{2+} alone were ineffective. In excised patches, the transitions $R \rightarrow R^S$ and $R' \rightarrow R''$ appeared to be irreversible. The attainment of state R'' protected from further desensitization.

1992). However, the two effects differ dramatically in that the catfish channel had a much higher sensitivity to Ca^{2+} and the effect was labile. These differences are considered further below. Ca^{2+}-dependent inhibition of photoreceptor CNG channel activation has also been reported. The cooperative binding of a fluorescent analog of cGMP was decreased by Ca^{2+} present in concentrations of 0.1–1 μM (Caretta, Cavaggioni, Grimaldi, and Sorbi, 1988). Recently, the Ca^{2+}-binding protein calmodulin was shown to decrease the affinity of cGMP for these channels (Hsu and Molday, 1993). It had previously been established that calmodulin is closely associated with the channel (Molday, Cook, Kaupp, and Molday, 1990). An effect like that described in Fig. 2 *A* was previously observed in the salamander photoreceptor CNG channel (Colamartino et al., 1991). Studying the same channels, Karpen, Loney, and

Baylor (1992) reported smaller CNG currents in patches excised into Ca^{2+}-containing, compared to Ca^{2+}-free solutions, which is also consistent with a Ca^{2+}-induced affinity reduction. Thus, Ca^{2+}-mediated shifts from high to low cyclic nucleotide affinity may be a common form of CNG channel regulation.

A recent study demonstrated that Ca^{2+}-dependent increases in cGMP affinity can also occur. Gordon et al., (1992) found that cGMP-gated channels in photoreceptor cells displayed a spontaneous sensitization with time that appeared to be due to a Ca^{2+}-activated phosphatase present at the internal membrane surface. Patches exposed to low Ca^{2+} for minutes lost the ability of spontaneous sensitization. Because spontaneous or divalent cation-induced sensitization were never observed in our experiments, such a phosphatase effect was unlikely to have contributed to the effects reported here. Ildefonse and collaborators (Ildefonse and Bennett, 1991; Ildefonse, Crouzy, and Bennett, 1992) reported that micromolar concentrations of certain divalent cations (Fe^{2+}, Ni^{2+}, Co^{2+}) induced a strong sensitization of photoreceptor CNG channels to activation by cGMP. However, Co^{2+}, which exerted a particularly potent effect at micromolar concentrations (Ildefonse and Bennett, 1991), had no effect in the concentration range 10 μM–1 mM used in the present study.

As illustrated in Fig. 7, the effect of Mg^{2+} is dependent on the sequence of channel preexposure to other divalent cations. This result suggests that other divalent cation effects on CNG channels may also be sequence-dependent. In addition, the use of Mg^{2+} to eliminate the cAMP affinity shift offers an opportunity to separate these effects from other types of divalent cation effects on CNG channels.

Possible Mechanism of Action

From the experiments described in this report, direct inhibitory effects of divalent cations on the CNG channel cannot be ruled out. However, recent studies (Kramer and Siegelbaum, 1992; Hsu and Molday, 1993) provide strong evidence for the existence of a regulatory protein in mediating the Ca^{2+}-induced inhibition. A regulatory protein, possibly calmodulin, may also have mediated the Ca^{2+}-induced effects in our system either directly (Hsu and Molday, 1993), or via a Ca^{2+}-activated calmodulin-dependent phosphodiesterase (Borisy et al., 1992). The sequence of divalent cation potency in reducing cAMP affinity ($Ca^{2+} > Sr^{2+} > Mn^{2+} > Ba^{2+} > Mg^{2+}$) corresponds closely to that required for the activation of calmodulin (Chao, Suzuki, Zysk, and Cheung, 1984). Another similarity is that Mg^{2+} also inhibited the Ca^{2+}-dependent affinity shift mediated by this enzyme (Hsu and Molday, 1993). Calmodulin also contains two classes of divalent cation binding sites, which corresponds to the minimum number required to explain the scheme in Fig. 7. However, it is not yet possible to reconcile all aspects of this model with the known properties of calmodulin. A potential problem is that the observed Ca^{2+}-sensitivity was about two orders of magnitude lower than required for calmodulin activation. On the other hand, the experiments described here were not a direct assay of calmodulin activation, and it is possible that if a limiting concentration of calmodulin was present in the excised patches, the apparent Ca^{2+}-sensitivity of the effect at the channel may have been skewed to much higher concentrations.

Kramer and Siegelbaum (1992) found no effect of either the calmodulin antagonist, calmidazolium, or of exogenous calmodulin application. However, because

calmodulin exerts multiple effects in olfactory neurons, these observations do not necessarily refute the hypothesis that calmodulin was involved. As well as a possible direct inhibitory effect on the olfactory CNG channel, calmodulin also activates olfactory adenylate cyclase (Anholt and Rivers, 1990; Frings, 1993) leading to an increase in cAMP levels, or a phosphodiesterase (Borisy et al., 1992), leading to a decrease. A particularly significant difference was that Kramer and Siegelbaum (1992) reported a strong time-dependent response rundown, whereas none was observed in the present study. It is difficult to attribute this to differences in experimental technique, because we used micro-patches from the apical knob, whereas they used mainly macro-patches, which should have reduced rundown rate, and indeed found an even greater rundown rate in micro-patches. The other significant difference was the higher Ca^{2+} concentration required in the present study. Taken together, these differences possibly suggest that the two effects are discrete, with the one reported here becoming evident at higher Ca^{2+} concentrations after washout of the effect reported by Kramer and Siegelbaum (1992).

It remains to be investigated why Mg^{2+}-induced protection did not occur either in intact cells or in naive patches. In excised patches, Mg^{2+}-induced protection was effective only after simultaneous Ca^{2+} and cAMP exposure (Fig. 7), such as the channels would normally experience during odorant stimulation in vivo. Thus, odorant exposure may change the regulatory protein-CNG channel complex in a way that would make itself susceptible to Mg^{2+} action in an excised patch. This implies the intervention of a cytosolic factor that is washed out after simulated odorant stimulation of excised patches.

Physiological Role

In isolated olfactory cells, both the odorant-induced and the cAMP-induced current display a desensitization which can be abolished by removing extracellular Ca^{2+} (Kurahashi, 1990; Kurahashi and Shibuya, 1990). This points to Ca^{2+} inflow as an important element in desensitization. Because in other systems, high (>100 μM) local Ca^{2+} concentrations can be generated at the internal surface of Ca^{2+}-permeant channels (Augustine and Neher, 1992; Llinas, Sugimori, and Silver, 1992), it is possible that the effect reported here may contribute significantly to the termination of olfactory signaling.

We thank Dr. T. Fabian for measuring concentrations of free Ca^{2+} in our solutions.

Supported by the Deutsche Forschungsgemeinschaft through SFB 246, project A10 and C1. J. W. Lynch was recipient of a CSIRO postdoctoral award and acknowledges the support of the CSIRO Sensory Research Centre, North Ryde, New South Wales, Australia.

Original version received 20 July 1992 and accepted version received 27 August 1993.

REFERENCES

Anholt, R. R. H., and A. M. Rivers. 1990. Olfactory transduction: crosstalk between second-messenger systems. *Biochemistry.* 29:4049–4054.

Augustine, G. J., and E. Neher. 1992. Calcium requirements for secretion in bovine chromaffin cells. *Journal of Physiology.* 450:247–271.

Bers, D. M. 1982. A simple method for the accurate determination of free [Ca] in Ca-EGTA solutions. *American Journal of Physiology.* 242:C404–C408.

Boekhoff, I., and H. Breer. 1992. Termination of second messenger signaling in olfaction. *Proceedings of the National Academy of Sciences, USA.* 89:471–474.

Borisy, F. F., G. V. Ronnett, A. M. Cunningham, D. Juilfs, J. Beavo, and S. H. Snyder. 1992. Calcium/calmodulin-activated phosphodiesterase expressed in olfactory receptor neurons. *Journal of Neuroscience.* 12:915–923.

Caretta, A., A. Cavaggioni, R. Grimaldi, and R. T. Sorbi. 1988. Regulation of cyclic GMP binding to retinal rod membranes by calcium. *European Journal of Biochemistry.* 177:139–146.

Chao, S.-H., Y. Suzuki, J. R. Zysk, and W. Y. Cheung. 1984. Activation of calmodulin by various metal cations as a function of ionic radius. *Molecular Pharmacology.* 26:75–82.

Colamartino, G., A. Menini, and V. Torre, V. 1991. Blockage and permeation of divalent cations through the cyclic GMP-activated channel from tiger salamander retinal rods. *Journal of Physiology.* 440:189–206.

Firestein, S., B. Darrow, and G. M. Shepherd. 1991. Activation of the sensory current in salamander olfactory receptor cells depends on a G-protein mediated cAMP second messenger system. *Neuron.* 6:825–835.

Frings, S. 1993. Protein kinase C sensitizes olfactory adenylate cyclase. *Journal of General Physiology.* 101:183–205.

Frings, S., J. W. Lynch, and B. Lindemann. 1992*a*. Properties of cyclic nucleotide-gated channels mediating olfactory transduction: activation, selectivity, and blockage. *Journal of General Physiology.* 100:45–67.

Lindemann, B., S. Frings, and J. W. Lynch. 1992. The cAMP-gated channel from olfactory sensory neurons of frog and rat: blockage by divalent ions, modelling of ionic diffusion with the Eyring approach, and modulation of sensitivity to cAMP. *European Neuroscience Association, Symposium: Channels regulated by intracellular nucleotides.* 15:2023*a*. (Abstr.)

Gordon, S. E., D. L. Brautigan, and A. L. Zimmerman. 1992. Protein phosphatases modulate the apparent agonist affinity of the light-regulated ion channel in retinal rods. *Neuron.* 9:739–748.

Hamill, O. P., A. Marty, E. Neher, B. Sakmann, and F. J. Sigworth. 1981. Improved patch-clamp techniques for high resolution current recording from cells and cell-free membrane patches. *Pflügers Archiv.* 391:85–100.

Hsu, Y.-E., and R. S. Molday. 1993. Modulation of the cGMP-gated channel of rod photoreceptor cells by calmodulin. *Nature.* 361:76–79.

Ildefonse, M., and N. Bennett. 1991. Single-channel study of the cGMP-dependent conductance of retinal rods from incorporation of native vesicles into planar lipid bilayers. *Journal of Membrane Biology.* 123:133–147.

Ilfedonse, M., S. Crouzy, and N. Bennett. 1992. Gating of retinal rod cation channel by different nucleotides: comparative study of unitary currents. *Journal of Membrane Biology.* 130:91–104.

Jan, L. Y., and Y. N. Jan. 1992. Structural elements involved in specific K^+ channel function. *Annual Review of Physiology.* 54:537–555.

Karpen, J. W., D. A. Loney, and D. A. Baylor. 1992. Cyclic GMP-activated channels of salamander retinal rods: spatial distribution and variation of responsiveness. *Journal of Physiology.* 448:257–274.

Kauer, J. S. 1987. Coding in the olfactory system. *In* Neurobiology of Taste and Smell. T. E. Finger and W. S. Silver, editors. John Wiley and Sons, Inc., New York. 205–231.

Kaupp, U. B., and K.-W. Koch. 1992. Role of cGMP and Ca^{2+} in vertebrate photoreceptor excitation and adaptation. *Annual Review of Physiology.* 54:153–175.

Kramer, R. H., and S. A. Siegelbaum. 1992. Intracellular Ca^{2+} regulates the sensitivity of cyclic nucleotide-gated channels in olfactory receptor neurons. *Neuron.* 9:897–906.

Kurahashi, T. 1990. The response induced by intracellular cyclic AMP in isolated olfactory receptor cells of the newt. *Journal of Physiology.* 430:355–371.

Kurahashi, T., and T. Shibuya. 1990. Calcium-dependent adaptive properties in the solitary olfactory receptor cells of the newt. *Brain Research.* 515:261–268.

Llinas, R., M. Sugimori, and R. B. Silver. 1992. Microdomains of high calcium concentration in a presynaptic terminal. *Science.* 256:677–679.

Lynch, J. W., and P. H. Barry. 1991. Properties of transient K^+ currents and underlying single K^+ channels in rat olfactory receptor neurons. *Journal of General Physiology.* 97:1043–1072.

Lynch, J. W., and B. Lindemann. 1992. Divalent cations decrease sensitivity of cAMP-gated channels to cAMP in rat olfactory receptor cells. *In* Xth Congress of European Chemosensory Research Organization (ECRO). 10:96*a*. (Abstr.)

Molday, L. L., N. J. Cook, U. B. Kaupp, and R. S. Molday. 1990. The cGMP-gated channel of bovine rod photoreceptor cells is associated with a 240-kDa protein exhibiting immunochemical cross-reactivity with spectrin. *Journal of Biological Chemistry.* 265:18690–18695.

Nakamura, T., and G. H. Gold. 1987. A cyclic nucleotide-gated conductance in olfactory receptor cilia. *Nature.* 325:442–444.

Nakatani, K., and K.-W. Yau. 1988. Calcium and magnesium fluxes across the plasma membrane of the toad rod outer segment. *Journal of Physiology.* 395:695–729.

Reed, R. R. 1992. Signalling pathways in odorant detection. *Neuron.* 8:205–209.

Yau, K.-W., and D. A. Baylor. 1989. Cyclic GMP-activated conductance of retinal rods. *Annual Review of Neuroscience.* 12:289–328.

Zufall, F., G. M. Shepherd, and S. Firestein. 1991. Inhibition of the olfactory cyclic-nucleotide gated ion channel by intracellular calcium. *Proceedings of the Royal Society of London, B. Biol. Sci.* 246:225–230.